Location of Parapapillary Gamma Zone and Vertical Fovea Location. The Beijing Eye Study 2011

Rahul A. Jonas,[1,2] Camilla F. Brandt,[3] Qi Zhang,[2] Ya X. Wang,[2] and Jost B. Jonas[2–4]

[1]Department of Ophthalmology, University Hospital of Cologne, Cologne, Germany
[2]Beijing Institute of Ophthalmology, Beijing Ophthalmology and Visual Sciences Key Laboratory, Beijing Tongren Hospital, Capital Medical University, Beijing, China
[3]Department of Ophthalmology, Medical Faculty Mannheim, Heidelberg University, Mannheim, Germany
[4]Institute of Molecular and Clinical Ophthalmology, Basel, Switzerland

Correspondence: Ya Xing Wang, Beijing Institute of Ophthalmology, Beijing Ophthalmology and Visual Sciences Key Laboratory, Beijing Tongren Hospital, Capital Medical University, 1 Dongjiaomin Lane, Dongcheng District, Beijing 100730, China;
yaxingw@gmail.com.

RAJ and CFB are joint first authors. YXW and JBJ are joint last authors.

Received: October 22, 2020
Accepted: December 3, 2020
Published: January 19, 2021

Citation: Jonas RA, Brandt CF, Zhang Q, Wang YX, Jonas JB. Location of parapapillary gamma zone and vertical fovea location. The Beijing Eye Study 2011. *Invest Ophthalmol Vis Sci.* 2021;62(1):18.
https://doi.org/10.1167/iovs.62.1.18

Purpose. To assess the spatial relationship between the locations of the parapapillary gamma zone and the fovea.

Methods. In a non-glaucomatous subgroup of the population-based Beijing Eye Study population, we measured the mean angle between the optic disc–fovea line and the horizontal (disc–fovea angle), the vertical distance of the fovea from the horizontal through the optic disc center (fovea vertical distance), and the location and width of the widest part of parapapillary gamma zone.

Results. The study included 203 individuals (203 eyes; mean axial length, 24.4 ± 1.5 mm; range, 22.03–28.87 mm). The widest gamma zone part was located most often temporal horizontally (51.7%), then inferiorly (43.8%), superiorly (2.5%), and nasally (2.0%). The disc–fovea angle (mean, 7.50° ± 4.00°; range, –6.30° to –23.25°) was significantly higher ($P = 0.003$; i.e., fovea located more inferiorly) in eyes with the widest gamma zone inferiorly (8.46° ± 4.37°) than in eyes with the widest gamma zone temporally (6.71° ± 3.46°) and in eyes with the widest gamma zone temporally, superiorly, or nasally combined (6.75° ± 3.53°; $P = 0.003$). The fovea vertical distance (mean, 0.65 ± 0.33 mm; range, –0.20 to 1.67 mm) was longer ($P = 0.001$; i.e., fovea located more inferiorly) in eyes with the widest gamma zone inferiorly (0.73 ± 0.33 mm) than in eyes with the widest gamma zone temporally (0.58 ± 0.30 mm) and in eyes with a temporal, superior, or nasal gamma zone combined (0.58 ± 0.31 mm; $P = 0.001$). The fovea vertical distance increased (multivariate analysis) with the widest gamma zone location inferiorly ($\beta = 0.25$; $P = 0.001$) and wider width of the gamma zone ($\beta = 0.19$; $P = 0.01$).

Conclusions. An inferior fovea location is associated with a wider inferior gamma zone and vice versa, supporting the notion of an inferior shifting of Bruch's membrane as the cause for an inferior gamma zone.

Keywords: parapapillary gamma zone, gamma zone, Bruch's membrane, Bruch's membrane opening, fovea, axial elongation, myopia

The optic nerve head canal consists anatomically of three layers: the Bruch's membrane opening (BMO), the opening in the choroidal layer delineated by the peripapillary border tissue of the choroid (Jacoby), and the scleral flange opening, covered by the lamina cribrosa and delineated by the peripapillary border tissue of the scleral flange (Elschnig).[1,2] Recent studies have revealed that, with axial elongation in moderately myopic eyes, the BMO shifts from its original position backward, usually into the temporal direction toward the fovea.[3] This leads to an overhanging of Bruch's membrane (BM) into the intrapapillary compartment at the nasal disc border, as well as a lack of BM in the temporal parapapillary region, referred to as a gamma zone.[3–5] Other studies have shown that the axial elongation-associated enlargement of the distance between the fovea and the optic disc is caused by the development and enlargement of a temporal gamma zone.[6] In contrast, the distance between the fovea and the border of BM at the peripheral margin of a gamma zone on the disc–fovea line is independent of axial length.[6] In a similar manner, the distance between the temporal superior arterial arcade and the temporal inferior arterial arcade as measured on a vertical line through the fovea is independent of axial length.[7] This observation led to the notion that BM at the posterior pole does not markedly enlarge in axially elongated eyes, unless macular BM defects have developed.[6,8,9] Correspondingly, the thickness of BM, in contrast to the thickness of the choroid and retina, does not decrease with longer axial length.[10–12] The concept of a shifting BM in axially elongating eyes can explain the dependence of the horizontal fovea position on the presence and size of a temporal gamma zone, with the horizontal fovea position measured as horizontal distance between the fovea and the optic disc.[8,9] Here we examined whether the vertical position of the fovea,

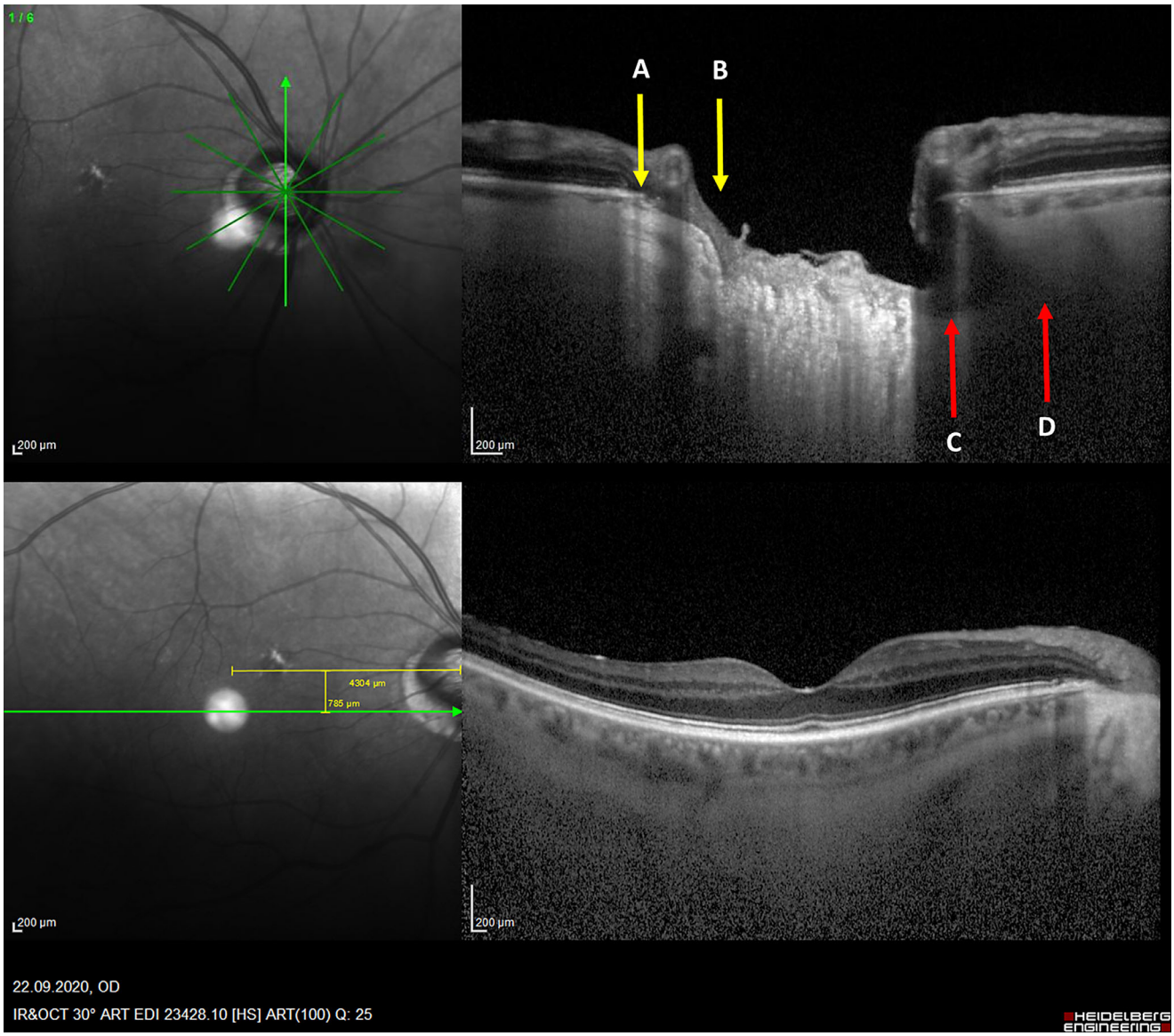

Figure 1. Vertical OCT image of the optic nerve head in an eye with an inferior gamma zone (between **A** and **B**), a corresponding overhanging of Bruch's membrane into the intrapapillary compartment at the superior optic disc border (between **C** and **D**), and a fovea location 0.78 mm inferior to the optic disc horizontal.

measured as the distance between the fovea and a horizontal line drawn through the optic disc center (fovea vertical distance) is also dependent on the location and size of the parapapillary gamma zone. The results may provide further information regarding the validity of the notion of a shifting of BM during the process of axial elongation.

Methods

The Beijing Eye Study 2011 was a population-based cross-sectional survey performed in Northern China. The Medical Ethics Committee of the Beijing Tongren Hospital approved the study protocol, and all participants gave informed written consent. Out of 4403 eligible individuals fulfilling the inclusion criteria of an age of 50+ years and living in rural or urban study regions, 3468 (78.8%) individuals participated. The mean age was 64.6 ± 9.8 years (range, 50–93 years). The study population and the study design have been described in detail previously.[3,13] We included in the present study the right eyes of individuals of an age-stratified, otherwise randomly selected subgroup of participants of the Beijing Eye Study population. Exclusion criteria for the present study were the presence of glaucomatous optic neuropathy, as the glaucomatous process might have changed the configuration of the optic nerve head, and unclear visualization of the BMO edges. Glaucoma was defined according to the optic nerve head criteria of the International Society of Geographic and Epidemiological Ophthalmology.[14,15] The inclusion criterion was the presence of a gamma zone.

All participants underwent a structured questionnaire including questions on the level of education, systemic examinations, and a comprehensive ophthalmic examination. The ophthalmic examination included measurement of visual acuity, slit-lamp examination of the anterior and posterior segment of the eye, and photography of the cornea, lens, optic disc, and macula (CR6-45NM fundus camera; Canon

Investigative Ophthalmology & Visual Science

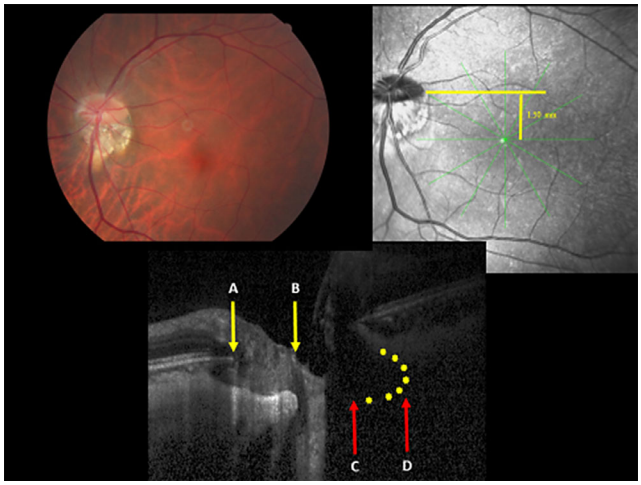

Figure 2. Vertical OCT image (inferior image) of the optic nerve head in an eye with an inferior gamma zone (between **A** and **B**), a corresponding overhanging of Bruch's membrane into the intrapapillary compartment at the superior optic disc border (between **C** and **D**), an angle between the disc–fovea line and the horizontal of 23.25°, and a fovea location 1.50 mm inferior to the optic disc horizontal.

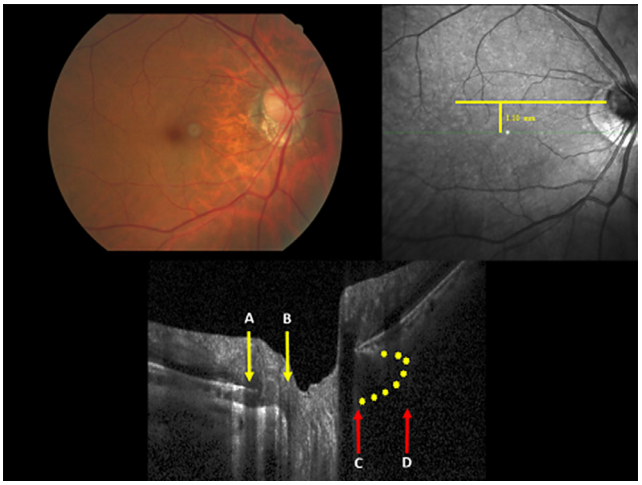

Figure 3. Vertical OCT image (inferior image) of the optic nerve head in an eye with an inferior gamma zone (between **A** and **B**), a corresponding overhanging of Bruch's membrane into the intrapapillary compartment at the superior optic disc border (between **C** and **D**), and a fovea location 1.1 mm inferior to the optic disc horizontal.

Inc., Tokyo, Japan). The optic nerve head including the peripapillary area was additionally imaged by spectral-domain optical coherence tomography (OCT) in enhanced depth imaging mode (Spectralis; Heidelberg Engineering, Heidelberg, Germany). The optic disc scan protocol included six radial scan lines with a scan length of 6 mm, centered on the optic disc, and each was comprised of 100 A-scans. The parapapillary region was examined with the intrinsic viewer (Heidelberg Eye Explorer 1.7.0.0 software; Heidelberg Engineering), which automatically synchronized the vertical lines of each B-scan and the infrared image taken by the OCT device. In eyes in which the end of BM did not reach the optic disc border (defined by the peripapillary border tissue of Elschnig), the parapapillary gamma zone was defined as the region between the end of BM and the border of the optic disc (Figs. 1–3). We measured the horizontal diameter and vertical diameter of the BMO, with the measurement lines running through the optic disc center, as well as the largest width of the gamma zone and its location in one of four parapapillary quadrants (i.e., temporal, superior, nasal, and inferior) (Figs. 1–3). Using the fundus photographs, we also measured the distance between the optic disc center and the foveola and the angle between the disc–fovea line and the horizontal.[6] If the foveola was located above the horizontal optic disc axis, the angle measurement was noted as a negative value. The technique of assessing the disc–fovea angle has already been described and applied in previous investigations by, for example, Lamparter et al.,[16] Denniss et al.,[17] Choi et al.,[18] and Kim et al.[19] The fovea vertical distance was trigonometrically calculated. To obtain the disc–fovea distance in real measurements, we corrected the magnification by the optic media of the eye and by the fundus camera using the Littmann and Bennett method.[20] As already described in detail, we additionally assessed the subfoveal choroidal thickness by OCT.[13,15]

Using a commercially available statistical software package (SPSS Statistics 25.0; IBM, Armonk, NY, USA), we first calculated the means and standard deviations, medians, and ranges of the main outcome parameters: disc–fovea angle, fovea vertical distance, and widest width of the gamma zone. In a second step, we performed a univariate analysis to assess associations among the main outcome parameters and other ocular parameters. In a third and final step, we carried out a multivariate analysis. We calculated the standardized regression coefficient (β), the non-standardized regression coefficient (B), and the 95% confidence intervals (CIs) of B. All P values were two sided and considered statistically significant when they were <0.05.

Results

The study included 203 eyes (203 individuals; 112 male, 55.2%) with a mean age of 61.6 ± 8.1 years (median, 60.0 years; range, 50–86 years) and a mean axial length of 24.4 ± 1.5 mm (median, 24.3 mm; range, 22.03–28.87 mm). The mean vertical diameter of BM opening was 1.79 ± 0.22 mm (median, 1.80 mm; range, 1.26–2.62 mm).

The maximal width of the gamma zone was located most often in the temporal horizontal quadrant (105 eyes, 51.7%), followed by the inferior quadrant (89 eyes, 43.8%), the superior quadrant (5 eyes, 2.5%), and the nasal quadrant (4 eyes, 2.0%) (Table 1). The mean disc–fovea angle was 7.50° ± 4.00° (median, 6.98°; range, –6.30° to –23.25°), the mean disc–fovea distance was 4.94 ± 0.34 mm (median, 4.97 mm; range, 3.86–5.99 mm), and the mean fovea vertical distance was 0.65 ± 0.33 mm (median, 0.61 mm; range, –0.20 to 1.67).

The disc–fovea angle was significantly higher ($P = 0.003$; i.e., fovea located more inferiorly) in eyes with the widest gamma zone located inferiorly (8.46° ± 4.37°) than in eyes with the widest gamma zone located temporally (6.71° ± 3.46°) and in eyes with the widest gamma zone located temporally, superiorly, or nasally combined (6.75° ± 3.53°; $P = 0.003$) (Table 1, Fig. 4).

If only eyes with a disc–fovea angle of less than 15° were included in the statistical analysis, similar results were obtained, with the disc–fovea angle being significantly associated with an inferior gamma zone location. The disc–fovea angle was larger ($P = 0.002$) in eyes with an inferior

Table 1. Morphometric Fundus Measurements Stratified by the Location of the Widest Parapapillary Gamma Zone in the Beijing Eye Study

		Mean ± SD							
				Bruch's Membrane Opening Diameter					
Widest Gamma Zone	***n* (%)**	**Age (y)**	**Axial Length (mm)**	**Horizontal (µm)**	**Vertical (µm)**	**Gamma Zone Width (µm)**	**Disc–Fovea Angle (°)**	**Disc–Fovea Distance (mm)**	**Fovea Vertical Distance (mm)**
Inferior quadrant	89 (43.8)	61.1 ± 7.8	24.2 ± 1.5	1566 ± 248	1805 ± 226	317 ± 201	8.46 ± 4.37	4.93 ± 0.34	0.73 ± 0.33
Temporal quadrant	105 (51.7)	62.1 ± 8.5	24.6 ± 1.4	1603 ± 214	1739 ± 223	319 ± 236	6.71 ± 3.46	4.95 ± 0.36	0.58 ± 0.30
Superior quadrant	5 (2.5)	60.6 ± 6.5	24.1 ± 2.0	1610 ± 99	1599 ± 193	260 ± 130	6.13 ± 4.07	4.88 ± 0.28	0.53 ± 0.37
Nasal quadrant	4 (2.0)	61.0 ± 7.5	23.1 ± 0.3	1456 ± 109	1911 ± 469	297 ± 252	8.53 ± 5.13	5.19 ± 0.14	0.77 ± 0.47
Temporal, superior, or nasal quadrant	114 (56.2)	62.0 ± 8.3	24.5 ± 1.4	1597 ± 208	1564 ± 183	315 ± 232	6.75 ± 3.53	4.96 ± 0.35	0.58 ± 0.31

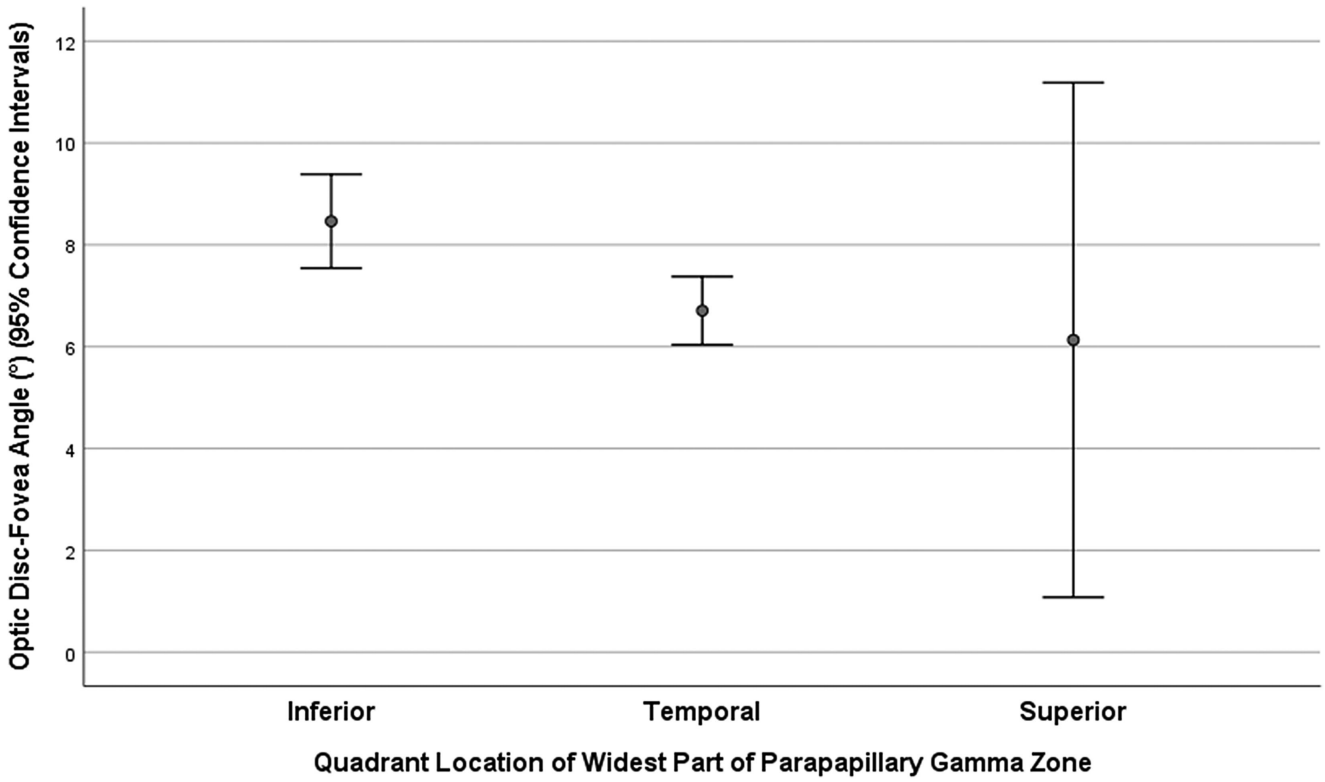

Figure 4. Graph showing the distribution of the disc–fovea angle (defined as the angle between the disc–fovea line and the horizontal) and the quadrant with the widest parapapillary gamma zone width.

location of the widest gamma zone (8.04° ± 3.93°) than in eyes with a temporal location of the widest gamma zone (6.40° ± 2.99°) and in eyes with the widest gamma zone located temporally, superiorly, or nasally combined (6.46° ± 3.11°; $P = 0.003$).

In multivariate regression analysis, the disc–fovea angle was associated with an inferior location of the widest gamma zone ($P = 0.001$) and with older age ($P = 0.008$), whereas, when added to the analysis, the parameters of gender ($P = 0.37$), region of habitation ($P = 0.07$), level of education ($P = 0.25$), axial length ($P = 0.66$), BMO diameter ($P = 0.24$), disc–fovea distance ($P = 0.11$), degree of fundus tessellation ($P = 0.46$), and subfoveal choroidal thickness ($P = 0.25$) were not significantly associated with the disc–fovea angle (Table 2).

The fovea vertical distance (mean, 0.65 ± 0.33 mm; median, 0.61 mm; range, –0.20 to 1.67) was significantly longer ($P = 0.001$; i.e., fovea located more inferiorly) in eyes with the widest gamma zone inferiorly (0.73 ± 0.33 mm) than in eyes with a widest gamma zone temporally (0.58 ± 0.30 mm) and in eyes with a temporal, superior, or nasal gamma zone combined (0.58 ± 0.31 mm; $P = 0.001$) (Fig. 5). In multivariate regression analysis, the fovea vertical distance increased with a location of the widest gamma zone inferiorly ($P = 0.001$) and a wider width of the gamma zone ($P = 0.01$). In that model, the fovea vertical distance was not associated with age ($P = 0.12$), gender ($P = 0.75$), region of habitation ($P = 0.29$), level of education ($P = 0.72$), axial length ($P = 0.96$), BMO diameter ($P = 0.51$), disc–fovea distance ($P = 0.62$), degree of fundus tessellation ($P = 0.32$), or subfoveal choroidal thickness ($P = 0.33$) (Table 2).

Discussion

In our study on eyes of healthy Chinese, the disc–fovea angle was significantly larger and the fovea vertical distance was significantly longer in eyes with the widest gamma zone in the inferior quadrant than in eyes with the widest gamma zone located in the temporal or superior quadrant. Correspondingly, the fovea vertical distance increased with a longer widest width of an inferior gamma zone and vice versa.

These findings agree with observations made in previous investigations, in which the disc–fovea distance increased with longer axial length parallel to the development and enlargement of a temporal gamma zone.[6] In contrast, the length of the macular BM, defined as the distance between the fovea and the border of BM at the peripheral edge of the temporal gamma zone, did not change.[6] Although in the previous study the horizontal fovea location defined as the distance from the optic disc was associated with a temporal gamma zone, the present investigation showed a spatial association between the vertical fovea location, defined as the distance of the fovea from the optic disc horizontal, and an inferior gamma zone. These finding support the hypothesis that BM moves backward during the process of axial elongation and myopization, leading to a backward shift of the BMO, usually in direction of the fovea (with subsequent development of a temporal gamma zone and secondary elongation of the disc–fovea distance). In some eyes, the BM shift may be directed more into the inferior–temporal direction, leading to a mainly inferior gamma zone and an inferior location of the fovea (Figs. 1–3). This notion is supported by

Investigative Ophthalmology & Visual Science

Table 2. Multivariate Regression Analysis of the Disc Fovea Angle to Multiple Parameters

	P	Standardized Correlation Coefficient (β)	Standardized Correlation Coefficient Squared (β^2)	Non-Standardized Correlation Coefficient (*B*)	95% CI
Disc–fovea-angle associated with ($P = 0.002$ for the whole model)					
Inferior gamma zone location	0.001	0.22	0.05	1.80	0.72, 2.88
Age (y)	0.008	0.18	0.03	0.09	0.02, 0.16
When added separately to the model					
Gender (male/female)	0.37	0.06	0.004	0.50	–0.60, 1.60
Region of habitation (rural/urban)	0.07	–0.13	0.02	–1.06	–2.19, 0.08
Level of education (1–5)	0.25	–0.08	0.006	–0.33	–0.89, 0.23
Axial length (mm)	0.66	0.03	0.0009	0.09	–0.30, 0.48
Bruch's membrane opening diameter (µm)	0.24	0.08	0.006	0.001	–0.001, 0.004
Disc–fovea distance (mm)	0.11	–0.11	0.01	–1.28	–2.83, 0.28
Fundus tessellation degree (0–3)	0.46	0.06	0.004	0.30	–0.50, 1.11
Subfoveal choroidal thickness (µm)	0.25	–0.09	0.008	–0.004	–0.009, 0.002
Vertical fovea distance from the optic disc horizontal associated with ($P < 0.001$ for the whole model)					
Inferior gamma zone location	0.001	0.25	0.06	0.17	0,07, 0.26
Gamma zone width (µm)	0.01	0.19	0.04	0.000	0,00, 0.00
When added separately to the model					
Age (y)	0.12	0.11	0.01	0.005	–0.001, 0.011
Gender (male/female)	0.75	0.02	0.0004	0.015	–0.079, 0.109
Region of habitation (rural/urban)	0.29	–0.08	0.006	–0.05	–0.15, 0.05
Level of education (1–5)	0.72	–0.03	0.0009	–0.01	–0.07, 0.05
Axial length (mm)	0.96	0.005	0.00003	0.001	–0.04, 0.05
Bruch's membrane opening diameter (µm)	0.51	0.05	0.003	0.00007	0.000, 0.000
Disc–fovea distance (mm)	0.62	–0.04	0.002	–0.04	–0.18, 0.11
Fundus tessellation degree (0–3)	0.32	0.08	0.006	0.04	–0.04, 0.11
Subfoveal choroidal thickness (µm)	0.33	–0.08	0.006	0.000	–0.001, 0.000

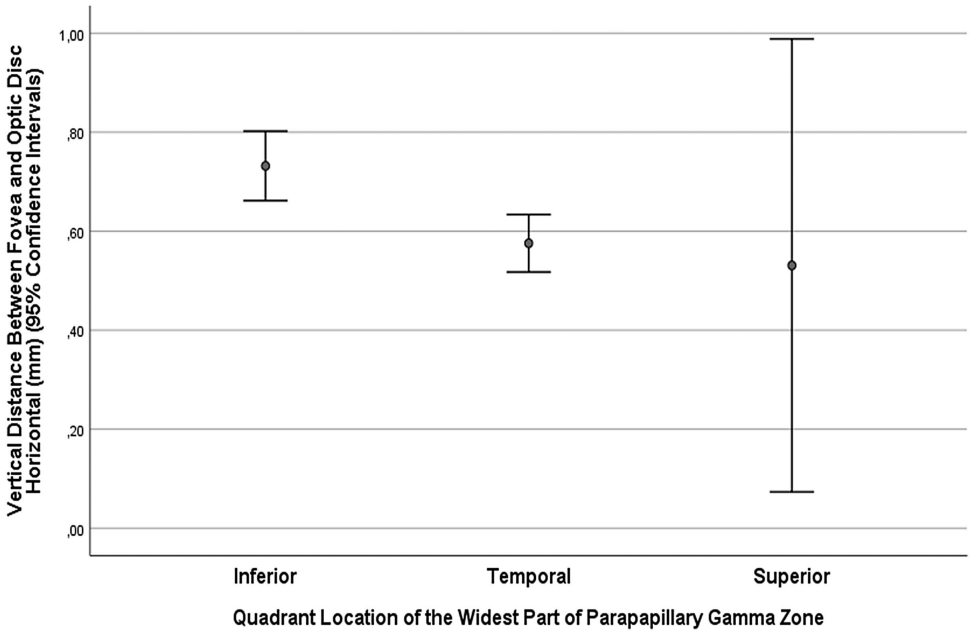

Figure 5. Graph showing the distribution of the vertical distance of the fovea from a horizontal line drawn through the optic disc center and the quadrant with the widest parapapillary gamma zone width.

the finding that the distance between the temporal superior vascular arcade and the temporal inferior vascular arcade does not change in axial elongation if eyes with macular BM defects are excluded.[7,8] This notion is also supported by the observation that the posterior choroid becomes thinner (more compressed) with more marked longer axial elongation.[21] The mechanism of a backward shift of BM could be explained by the assumption that the axial elongation occurs due to enlargement of BM in the equatorial region. By such a mechanism, the eye would predominantly become longer and would enlarge only to a minor degree in the coronal diameters. During myopization, the globe does, indeed, change its shape from a mostly spherical configuration to a prolate shape or to a tube-like shape with two half-spheres at both of its ends.[8,22,23] This observation fits with histomorphometric findings that, in the equatorial region, retinal thickness and the density of the retinal pigment epithelium (RPE) cells decrease with longer axial length, whereas at the posterior pole retinal thickness, RPE density and choriocapillaris thickness are mostly independent of axial length.[24–26] The notion of BM having biomechanical importance in the process of axial elongation is supported by the observation that the stiffness of BM is comparable to or higher than the stiffness of other ocular tissues and that BM can sustain a relatively high pressure before rupture.[27]

An alternative to BM as the primary tissue elongating the eye is the sclera, as BM and sclera are the only biomechanically strong tissue layers. The choroid and the retina are biomechanically too weak in their structures to force the other ocular tissue layers to expand. If the eye wall enlargement occurred primarily by an enlargement of the midperipheral sclera, the choroidal space at the posterior pole would widen, and the peripapillary scleral flange opening (i.e., the lamina cribrosa) in the optic nerve canal would move backward. This would lead to an oblique course of the optic nerve canal from the nasal inner layer to the temporal outer layer. Neither of these morphological features, however, is found in myopic eyes, in which the choroid at the posterior pole progressively becomes thinner with axial elongation and the course of the optic nerve canal runs from the temporal inner layer to the nasal outer layer. These findings support BM, in contrast to the sclera, as being the primary tissue elongating the globe during myopization. There are additional findings favoring BM as the primary tissue elongating the globe in myopia. The process of emmetropization (and potentially the process of myopization as an overshooting of the process of emmetropization) is the adaptation of the length of the optical axis depending on the given optical properties of the cornea and lens. The optical axis ends at the photoreceptor outer segments in close proximity to the BM, whereas the sclera is separated from the photoreceptor outer segments by the choroid, the thickness of which fluctuates between morning and evening and is additionally dependent on other parameters. It may make it unlikely that the sclera could determine the length of the optical axis with a precision of approximately 100 µm. The notion of an enlargement of the globe in the equatorial region during the process of emmetropization and myopization fits with the observation that the afferent sensory part of the feedback mechanism is located in the equatorial and retro-equatorial regions.[28] Studies have shown that a peripheral defocus leads to axial elongation.

Because the RPE, through its basal membrane, is relatively firmly connected with BM, any movement of the posterior BM may result in a corresponding movement of the fovea. In the case of eyes with an inferior or inferior temporal gamma zone (and a corresponding overhanging of BM into the intrapapillary compartment at the superior to nasal superior disc region), the enlargement of BM in the equatorial region might be more marked in the superior region than in the inferior region. This would lead to a surplus of BM in the superior hemisphere, resulting in a shift of the BMO inferiorly. Because the BMO and the fovea are both based on BM, movement of BM in the inferior direction would result

Investigative Ophthalmology & Visual Science

in an inferior location of the fovea in spatial association with an inferior location of the BMO, which results in an inferior gamma zone.

The measurement of the mean fovea location of about 0.65 ± 0.33 mm agrees with the results of a previous study in which the same parameter was measured on fundus photographs and a mean value of 0.53 ± 0.34 mm inferior to the horizontal optic disc axis.[29]

The findings obtained in our study may have several clinical implications. The position of the blind spot in the visual field depends on the spatial relationship between the fovea and optic nerve head. The results of our study suggest that the blind spot may be located more inferiorly in eyes with an inferior gamma zone compared to eyes without a superior gamma zone. In particular, in automated perimetry, such an abnormal spatial relationship between the visual center and the blind spot may influence the description of visual field defects. Second, previous studies have shown that the position of the peaks in the peripapillary retinal nerve fiber layer thickness profile depends on the spatial relationship between the optic disc and fovea.[16–18,30] According to the current study, eyes with an inferior gamma zone and inferiorly located fovea may have a different position of the retinal nerve fiber layer peaks than eyes with a superior gamma zone.

When discussing the results of our study, its limitations should be considered. First, although the primary recruitment of the study participants followed a population-based system, the current study consists of a subgroup of randomly chosen individuals with gamma zones and without disorders of the optic nerve and macula. Second, the study population consisted of only Chinese, so the results may not transfer directly to other ethnicities. Third, only the location of the widest gamma zone position was taken into account in this study, so that an eye with a circumpapillary gamma zone with the widest gamma zone located inferiorly fell into the same category as an eye with a small gamma zone with its widest part located inferiorly. To partially compensate for this weakness in the study design, we also measured the width of the widest gamma zone part and found that this parameter correlated with the fovea vertical distance (Fig. 5).

Fourth, one may argue that gamma zones are present mainly in highly myopic eyes and that the mean axial length of the participants of our study was almost normal (24.4 ± 1.5 mm). The question may arise, then, as to why many of the study participants had a gamma zone without being highly myopic. Although gamma zones are largest in highly myopic eyes, the majority of moderately myopic eyes show a gamma zone of moderate size. It has been suggested that, in eyes that are not highly myopic, gamma zones (located most often in the temporal region) are due to a shift in the BMO in the direction of the fovea and that the width of a gamma zone on the temporal side corresponds to the length of the overhanging part of BM at the nasal side of the optic disc.[3] In highly myopic eyes, with a cutoff value of about 26.5 mm of axial length, the BMO enlarges so that eventually the nasally overhanging part of BM retracts and a circular gamma zone develops.[3] Because the circular enlargement of the BMO may not be due to a shift of BM but instead could be due to an increase in the strain within BM, highly myopic eyes with a circular gamma zone may not be useful for assessing a relationship between a shift of BM and the position of the fovea.[31] The only moderately myopic range of axial length of our study population may therefore support the appropriateness of the study population for this study's goals.

Fifth, the largest disc–fovea angle in the study population was relatively large (23.2°) (Fig. 2), so that one may argue that some extreme outlier cases could have distorted the results of the statistical analyses. If, however, eyes with a disc–fovea angle of ≥15° were excluded from the statistical analysis, then the results remained mostly unchanged. Finally, one may also argue that a temporal gamma zone could cause a more temporal location of the fovea, which would then lead to a divergent pseudostrabismus; however, the development of a divergent pseudostrabismus in myopic eyes has not been detected for the majority of myopic eyes. It is more likely that the assumed process of BM enlargement in the equatorial region occurs in all meridians in a more or less symmetric manner, so that the posterior pole with the fovea in its center is equally pushed backward (resulting in a compression and thinning of the posterior choroid) without a marked change in the position of the fovea in the center of the posterior pole.

In conclusion, the vertical position of the fovea measured as vertical distance from the optic disc horizontal is associated with an inferior gamma zone and increases with a larger inferior gamma zone width. It supports the notion of a shifting of BM, with an inferior gamma zone caused by a downward shift of the BMO. This leads to a misalignment of the BMO compared with the choroidal opening and the peripapillary scleral flange opening (lamina cribrosa) of the optic nerve head canal and is accompanied by an inferior shift of the fovea.

Acknowledgments

Supported by the National Natural Science Foundation of China (81570835).

Disclosure: **R.A. Jonas,** European and US patent holder (16 720 043.5 and US 2019 0085065 A1, Agents for use in the therapeutic or prophylactic treatment of myopia or hyperopia) (P); **C.F. Brandt,** None; **Q. Zhang,** None; **Y.X. Wang,** None; **J.B. Jonas,** European and US patent holder (16 720 043.5 and US 2019 0085065 A1, Agents for use in the therapeutic or prophylactic treatment of myopia or hyperopia) (P), US patent application (Agents for the use in the therapeutic or prophylactic treatment of retinal pigment epithelium associated diseases) (P), Biochemicals UK, Ltd., patent holder (20120263794, Treatment of eye diseases using encapsulated cells encoding and secreting neuroprotective factor and/or anti-angiogenic factor) (P), Novartis (F)

References

1. Jonas JB, Ohno-Matsui K, Panda-Jonas S. Myopia: anatomic changes and consequences for its etiology. *Asia Pac J Ophthalmol (Phila)*. 2019;8(5):355–359.
2. Jonas RA, Holbach L. Peripapillary border tissue of the choroid and peripapillary scleral flange in human eyes. *Acta Ophthalmol*. 2020;98(1):e43–e49.
3. Zhang Q, Xu L, Wei WB, Wang YX, Jonas JB. Size and shape of Bruch's membrane opening in relationship to axial length, gamma zone and macular Bruch's membrane defects. *Invest Ophthalmol Vis Sci*. 2019;60(7):2591–2598.
4. Jonas JB, Jonas SB, Jonas RA, et al. Parapapillary atrophy: histological gamma zone and delta zone. *PLoS One*. 2012;7(10):e47237.
5. Jonas JB, Ohno-Matsui K, Spaide RF, Holbach L, Panda-Jonas S. Macular Bruch's membrane defects and axial length: association with gamma zone and delta zone

in peripapillary region. *Invest Ophthalmol Vis Sci*. 2013;54(2):1295–1302.
6. Jonas RA, Wang YX, Yang H, et al. Optic disc - fovea distance, axial length and parapapillary zones. The Beijing Eye Study 2011. *PLoS One*. 2015;10(9):e0138701.
7. Jonas JB, Weber P, Nagaoka N, Ohno-Matsui K. Temporal vascular arcade width and angle in high axial myopia. *Retina*. 2018;38(9):1839–1847.
8. Jonas JB, Ohno-Matsui K, Jiang WJ, Panda-Jonas S. Bruch membrane and the mechanism of myopization. A new theory. *Retina*. 2017;37(8):1428–1440.
9. Panda-Jonas S, Xu L, Yang H, Wang YX, Jonas SB, Jonas JB. Optic disc morphology in young patients after antiglaucomatous filtering surgery. *Acta Ophthalmol*. 2014;92(1):59–64.
10. Jonas JB, Holbach L, Panda-Jonas S. Bruch's membrane thickness in high myopia. *Acta Ophthalmol*. 2014;92(6):e470–e474.
11. Bai HX, Mao Y, Shen L, et al. Bruch's membrane thickness in relationship to axial length. *PLoS One*. 2017;12(8):e0182080.
12. Dong L, Shi XH, Kang YK, et al. Bruch's membrane thickness and retinal pigment epithelium cell density in experimental axial elongation. *Sci Rep*. 2019;9(1):6621.
13. Wang YX, Xu L, Wei WB, Jonas JB. Intraocular pressure and its normal range adjusted for ocular and systemic parameters. The Beijing Eye Study 2011. *PLoS One*. 2018;13(5):e0196926.
14. Foster PJ, Buhrmann R, Quigley HA, Johnson GJ. The definition and classification of glaucoma in prevalence surveys. *Br J Ophthalmol*. 2002;86(2):238–242.
15. Wang YX, Xu L, Yang H, Jonas JB. Prevalence of glaucoma in North China. The Beijing Eye Study. *Am J Ophthalmol*. 2010;150(6):917–924.
16. Lamparter J, Russell RA, Zhu H, et al. The influence of intersubject variability in ocular anatomical variables on the mapping of retinal locations to the retinal nerve fiber layer and optic nerve head. *Invest Ophthalmol Vis Sci*. 2013;54(9):6074–6082.
17. Denniss J, Turpin A, Tanabe F, Matsumoto C, McKendrick AM. Structure-function mapping: variability and conviction in tracing retinal nerve fiber bundles and comparison to a computational model. *Invest Ophthalmol Vis Sci*. 2014;55(2):728–736.
18. Choi JA, Kim JS, Park HY, Park H, Park CK. The foveal position relative to the optic disc and the retinal nerve fiber layer thickness profile in myopia. *Invest Ophthalmol Vis Sci*. 2014;55(3):1419–1426.
19. Kim KE, Jeoung JW, Park KH, Kim DM, Kim SH. Diagnostic classification of macular ganglion cell and retinal nerve fiber layer analysis: differentiation of false-positives from glaucoma. *Ophthalmology*. 2015;122(3):502–510.
20. Bennett AG, Rudnicka AR, Edgar DF. Improvements on Littmann's method of determining the size of retinal features by fundus photography. *Graefes Arch Clin Exp Ophthalmol*. 1994;232(6):361–367.
21. Wei WB, Xu L, Jonas JB, et al. Subfoveal choroidal thickness: the Beijing Eye Study. *Ophthalmology*. 2013;120(1):175–180.
22. Heine L. Beiträge zur Anatomie des myopischen Auges. *Arch Augenheilkd*. 1899;38:277–290.
23. Jonas JB, Ohno-Matsui K, Holbach L, Panda-Jonas S. Association between axial length and horizontal and vertical globe diameters. *Graefes Arch Clin Exp Ophthalmol*. 2017;255(2):237–242.
24. Jonas JB, Ohno-Matsui K, Holbach L, Panda-Jonas S. Retinal pigment epithelium cell density in relationship to axial length in human eyes. *Acta Ophthalmol*. 2017;95(1):e22–e28.
25. Jonas JB, Xu L, Wei WB, et al. Retinal thickness and axial length. *Invest Ophthalmol Vis Sci*. 2016;57(4):1791–1797.
26. Panda-Jonas S, Holbach L, Jonas JB. Choriocapillaris thickness and density in axially elongated eyes [published online ahead of print June 19, 2020]. *Acta Ophthalmol*, https://doi.org/10.1111/aos.14486.
27. Wang X, Teoh CKG, Chan ASY, Thangarajoo S, Jonas JB, Girard MJA. Biomechanical properties of Bruch's membrane-choroid complex and their influence on optic nerve head biomechanics. *Invest Ophthalmol Vis Sci*. 2018;59(7):2808–2817.
28. Smith EL, Hung LF, Huang J, Blasdel TL, Humbird TL, Bockhorst KH. Effects of optical defocus on refractive development in monkeys: evidence for local, regionally selective mechanisms. *Invest Ophthalmol Vis Sci*. 2010;51(8):3864–3873.
29. Jonas JB, Nguyen NX, Naumann GOH. The retinal nerve fiber layer in normal eyes. *Ophthalmology*. 1989;96(5):627–632.
30. Jonas RA, Wang YX, Yang H, et al. Optic disc - fovea angle: the Beijing Eye Study 2011. *PLoS One*. 2015;10(11):e0141771.
31. Jonas JB, Ohno-Matsui K, Jiang WJ, Panda-Jonas S. Bruch membrane and the mechanism of myopization. A new theory. *Retina*. 2017;37(8):1428–1440.

Investigative Ophthalmology & Visual Science